Available online at www.sciencedirect.com
SCIENCE DIRECT®
Radiation Measurements 40 (2005) 560–568
Radiation Measurements
www.elsevier.com/locate/radmeas

Long-term measurements of radon progeny concentrations with solid-state nuclear track detectors

K.N. Yu[a,*], D. Nikezic[a,1], F.M.F. Ng[a], J.K.C. Leung[b]

[a]*Department of Physics and Materials Science, City University of Hong Kong, Tat Chee Avenue, Kowloon Tong, Kowloon, Hong Kong, Hong Kong*
[b]*Department of Physics, University of Hong Kong, Pokfulam Road, Hong Kong, Hong Kong*

Received 27 August 2004; received in revised form 8 January 2005; accepted 3 March 2005

Abstract

In this paper, we review existing methods for long-term measurements of radon decay products with solid-state nuclear track detectors. We then propose a method to determine the equilibrium factor using the bare LR 115 detector. The partial sensitivities p_i of the LR 115 detector to ^{222}Rn and its α-emitting short-lived progeny, ^{218}Po and ^{214}Po, were investigated. We determined the distributions of lengths of major and minor axes of the perforated α-tracks in the LR 115 detector produced by ^{222}Rn, ^{218}Po and ^{214}Po through Monte Carlo simulations. The track parameters were first calculated using a track development model with a published V function, and by assuming a removed active layer of 6.54 μm. The distributions determined for different α-emitters were found to be completely overlapping with one another. This implied equality of partial sensitivities for radon and its progeny.

Equality of partial sensitivities makes convenient measurements of a proxy equilibrium factor F_p possible which is defined in the present work as $(f_1 + f_3)$ and is equal to the ratio between the sum of concentrations of the two α-emitting radon progeny (^{218}Po + ^{214}Po) to the concentration of radon gas (^{222}Rn). In particular, we have found $F_p = (\rho/\rho_i t C_0) - 1$, where ρ (track/m^2) is the total track density on the detector, $\rho_i = 0.288 \times 10^{-2}$ m (for the V function mentioned above and for a removed active layer of 6.54 μm), t is the exposure time and C_0 (Bq/m^3) is the concentration of ^{222}Rn. If C_0 is known (e.g., from a separate measurement), we can obtain F_p. The proxy equilibrium factor F_p is also found to be well correlated with the equilibrium factor between radon gas and its progeny through the Jacobi room model. This leads to a novel method for long-term determination of the equilibrium factor.

Experimental irradiation of LR 115 detectors to known ^{222}Rn concentrations as well as known equilibrium factors were carried out to verify the present method. The relationship between ρ_i and the removed layer was then derived for the V function specifically determined for the LR 115 detectors we were using for the experiments. The actual removed layers for individual detectors after etching were measured accurately using surface profilometry. A curve showing the relationship between the removed layer and the track diameter of normally incident 3 MeV α-particles is also provided for other researchers, who do not have access to surface profilometry, to use the present technique conveniently.

Keywords: Radon progeny concentration; Equilibrium factor; LR 115 detector

*Corresponding author. Tel.: +852 27887812; fax: +852 27887830.
E-mail address: peter.yu@cityu.edu.hk (K.N. Yu).
[1]On leave from Faculty of Sciences, University of Kragujevac, Serbia and Monte Negro.

1350-4487/$ - see front matter © 2005 Elsevier Ltd. All rights reserved.
doi:10.1016/j.radmeas.2005.03.007

1. Introduction

Inhaled radon (^{222}Rn) progeny are the most important source of irradiation of the human respiratory tract. Epidemiological studies of underground miners of uranium and other minerals have provided reasonably firm estimates of the risk of lung cancer associated with exposure to radon progeny (e.g., Lubin et al., 1995; Muirhead, 1997; NRC, 1999).

Methods for long-term monitoring of the ^{222}Rn gas itself are well established, such as through the use of solid-state nuclear track detectors (SSNTDs) (see e.g., Nikolaev and Ilic (1999) for a survey). When α-particles strike a SSNTD, latent tracks will be formed, which will become visible under the optical microscope on suitable chemical etching. However, methods for long-term monitoring of the concentrations of radon progeny, or the equilibrium factor (which surrogates the ratios of concentrations of radon progeny to the concentration of the ^{222}Rn gas), are still being explored. The equilibrium factor of radon progeny is calculated as

$$F_{^{222}\mathrm{Rn}} = 0.105 f_{^{218}\mathrm{Po}} + 0.515 f_{^{214}\mathrm{Pb}} + 0.380 f_{^{214}\mathrm{Bi,Po}}, \quad (1)$$

where f_i is the ratio of the activity concentration of the ith radon decay product to that of ^{222}Rn, i.e., $f_1 = f_{^{218}\mathrm{Po}}$, $f_2 = f_{^{214}\mathrm{Pb}}$ and $f_3 = f_{^{214}\mathrm{Bi,Po}}$.

2. Critical analysis of existing methods for long-term measurements of radon progeny with SSNTD

Recently, Amgarou et al. (2003) and Nikezic and Yu (2004) made surveys of existing methods for determining the equilibrium factor and radon progeny concentrations and concluded that all methods suffered from some problems. Here we will give some more detailed description of the methods and problems involved.

The first method was proposed by Frank and Benton (1977). In this method, cellulose nitrate detectors were used, one in a diffusion chamber and the other as an open detector. The open detector registers the total concentration of α-particle-emitting nuclei in air, i.e., ^{222}Rn + progeny (^{218}Po + ^{214}Po), while the closed detector measures only ^{222}Rn. The ratio between the readings for the open and closed detectors is related to the equilibrium factor and from here it should be possible to estimate the equilibrium factor. This method was used by many authors under different detector setups, but did not give realistic results. This method assumed the same sensitivities for the open and closed detectors for each of the α-emitting nuclei in the ^{222}Rn decay chain. This assumption is not correct because the sensitivity of the closed detector depends on the chamber shape and dimension as well as other construction details, and may be very different from the sensitivity of an open detector.

Another method was proposed by Fleischer (1984) who used four detectors for radon progeny measurements. Three detectors were covered with polyethylene absorber foils with different thickness. The bare detector and the first one with a 20 μm absorber can detect α-particles emitted by ^{222}Rn and the progeny ^{218}Po + ^{214}Po. The other two with thicker absorbers measure α-emissions from ^{218}Po + ^{214}Po and ^{214}Po. By this method, the α-active progeny (^{218}Po and ^{214}Po) could be measured separately. However, this method fails because of unavoidable progeny deposition on the detectors and on the absorber foils. The amount of deposition is not known, and may be variable. The deposited progeny have much larger detection probability and this significantly affects the progeny measurements.

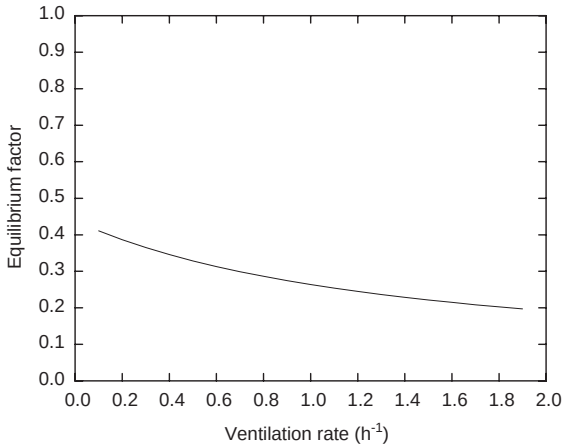

Fig. 1. Equilibrium factor as a function of the ventilation rate. Other parameters: aerosol attachment rate $\lambda_a = 50\,h^{-1}$, deposition rate of unattached progeny $\lambda_{d,u} = 20\,h^{-1}$ and deposition rate of attached progeny $\lambda_{d,a} = 0.2\,h^{-1}$, recoil factor 0.83.

A second group of methods is based on the assumption that the equilibrium factor depends mainly on the ventilation rate. In fact, several processes affect the concentration ratio of progeny to radon, such as deposition and ventilation. The model of Jacobi (1972) describes the balance of radon and its progeny in a closed space. If all other parameters are kept at their best estimates, from the ratio of the track density on the open and closed detectors, one could infer the ventilation rate and the equilibrium factor (Planinic and Faj, 1990). However, this method fails for two reasons. The first one is that the equilibrium factor is a weak function on the ventilation rate. Actually, the radon concentration is very dependent on the ventilation rate, but the ratio of progeny concentrations to the radon concentration is not. The dependence of the equilibrium factor on the ventilation rate is shown in Fig. 1.

For nominal ventilation rates between 0.5 and 1.5 h^{-1}, the equilibrium factor varies between 0.32 and 0.23 (if other parameters are kept constant). This change is relatively small, and if we take into account other uncertainties, such as statistical errors in the number of the tracks, etc., the determination of the equilibrium factor through measurements of the ventilation rate becomes problematic. Another reason

why this method fails is that the deposition rates of radon progeny can be very different from the "typical" values. Another deficiency of the method is the assumption on equal sensitivities of the open and closed detectors.

One extension of this method was proposed by Dorschel and Piesch (1993). In this method, special etching conditions have to be applied on the track detector so that the energy window is between 6.05 and 7.5 MeV. In this way, only ^{214}Po in air was measured. From the ratio $f_{^{214}\mathrm{Po}}$ of concentrations between ^{214}Po and ^{222}Rn, one can obtain the equilibrium factor. This method was also based on the assumption that all other parameters were kept at their best estimations except the ventilation rate. This method is better than the previous one, because the equilibrium factor is better correlated to $f_{^{214}\mathrm{Po}}$ than to the track density ratio between the open and closed detectors, but there are difficulties to realize such a narrow energy window. The calibration is also a problem because it is not easy to obtain air contaminated only with ^{214}Po whose concentration should be known. Here, the calibration factor has to be calculated.

Nikezic and Baixeras (1996) proposed the barrier method for which barriers were placed at some distances in front of LR 115 detectors. Due to the differences in the α-energies emitted from different progeny and the existence of an upper limit in the energy window for the LR 115 detector, separation of progeny has been shown to be theoretically possible. An α-particle has to travel some distance in the air before its energy falls below the upper limit in the energy window to be detected. If the barrier is too close, the LR 115 detector will not detect any α-particle. If the barrier is a little bit farther away, it will detect α-particles from the radon only, and so on. However, experimental verification of this method was not successful because of plateout of radon progeny on the barrier, for which the theoretical model failed to describe.

Another class of methods is based on spectrometry of α-particles. From the track parameters, it is possible to determine the energy of α-particles that produce the tracks. However, the track parameters are dependent on the incident angle in addition to the incident energy. Therefore, the same track parameters (major and minor axes) can be obtained with different incident energies. Other track parameters are needed, such as the average gray level or the track shape. Even the establishment of the incident α-particle spectrum from the track parameters is difficult by itself and tedious. The second step would be the interpretation of the data and linking the obtained spectra with the equilibrium factors or to the concentration of particular radon progeny. The incident α-particle spectrum depends on the relative concentrations of radon progeny in air. In Fig. 2, incident α-particle spectra are given, where $f(E)$ refers to the fraction of α-particles incident on the open detector with an energy between E and $E + \mathrm{d}E$ (Nikezic and Yu, 2002).

In Fig. 2, the spectra for two extreme cases are given, namely, for an equilibrium factor $F = 1$ and for a low equilibrium factor $F = 0.1$. The curves in Fig. 2 show a non-Gaussian peak at 5.49 MeV and cutoff structures above

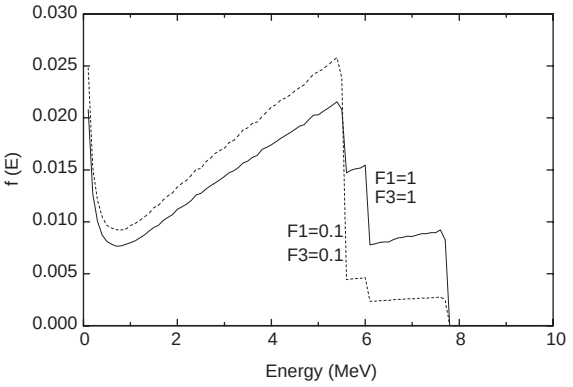

Fig. 2. Incident α-particle spectra for two extreme ratios of progeny to radon concentrations (Nikezic and Yu, 2002).

5.49 MeV. The first cutoff from right to left is related to ^{214}Po while the second to ^{218}Po. The curves have plateaus between 6 and 7.69 MeV and between 5.49 and 6 MeV; the former (^{214}Po plateau) is wider because of the wider energy gap, while the latter (^{218}Po plateau) is narrower and higher than the ^{214}Po plateau. By analyzing the height of these two plateaus, one can infer some information about the relative activities of ^{218}Po and ^{214}Po. If their activities are equal (as shown in Fig. 2, where $F1 = F3$), the ^{218}Po plateau is two times higher than the ^{214}Po plateau.

The process of plateout will create two intensive peaks at 6 and 7.69 MeV in the measured spectrum. The heights of these peaks depend on the amount of plateout as well as the efficiency and energy resolution of the detector and the measuring conditions. The most important part of the spectrum is between 6 and 7.69 MeV. Here, only ^{214}Po from air contributes to the detector response. In order to avoid the influence of plateout (if SSNTDs are considered), the energy window between 6.2 and 7.5 should be considered. Actually the width of the window depends on the energy resolution attainable in measurements, but of course, it should not be wider than the range from 6–7.69 MeV. If the energy resolution is worse than 1 MeV, measurements of radon progeny would not be possible by analyzing the energy spectrum. The feasibility of radon progeny measurement relies on the provision of high-resolution α spectroscopy.

If only ^{214}Po is measured, the equilibrium factor is not yet readily available. One extension of the spectroscopy method is to measure only tracks with the ratio of major to minor axes in some ranges, so that only particles that enter the detector with an angle close to normal incidence are counted (Hadler and Paulo, 1994). In Fig. 3, the angular distribution of incident α-particles is given. From this figure, it is clear that a very small number of particles will hit the detector with an angle close to 90°. Therefore, the method mentioned above has to be very tedious since the number of tracks satisfying the given condition is rather small. Although the tediousness can be resolved by using

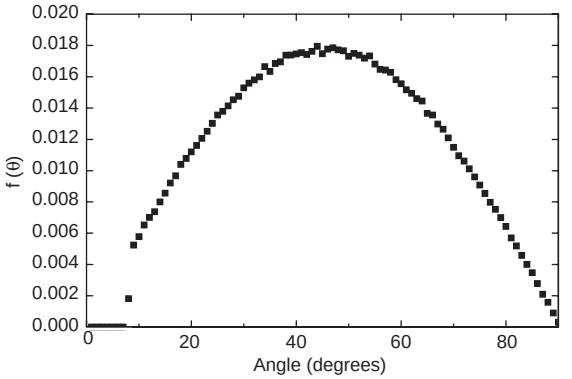

Fig. 3. Angular distribution of incident α-particles onto the detector (Nikezic and Yu, 2002).

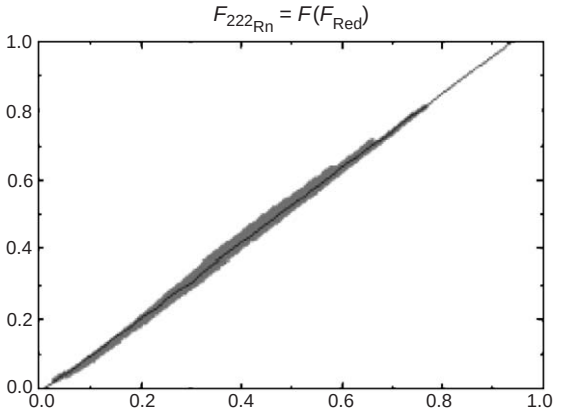

Fig. 4. The ^{222}Rn progeny equilibrium factor expressed as a function of the reduced equilibrium factor, calculated for all possible values for the parameters in the Jacobi model (Amgarou et al., 2003).

automatic image analysis systems, the low sensitivity caused by the selection of the tracks is an intrinsic limitation.

From the above discussion, it can be seen that up to now there is still no very accurate, practical and widely used methods for long-term measurements of the equilibrium factor with nuclear track detectors. All of the above-mentioned methods suffer from some kind of problems. New ideas and novel proposals are needed in this field. A most recent one is given by Amgarou et al. (2003) who proposed measurements of the equilibrium factor through the so-called "reduced" equilibrium factor, which is defined as

$$F_{\mathrm{Red}} = 0.105 f_{^{218}\mathrm{Po}} + 0.380 f_{^{214}\mathrm{Bi,Po}}, \quad (2)$$

where f_i is the ratio of the concentrations between the ith progeny and radon.

Employment of three detectors was proposed in the application of this method. The first one was closed inside a diffusion chamber, which measured radon only. Two open detectors were used with different energy windows for separate measurements of ^{218}Po and ^{214}Po. The etching conditions applied to the Makrofol detectors for the required energy window were also determined. The reduced equilibrium factor F_{Red} was then calculated. It was further shown that the total equilibrium factor depended on F_{Red} in a very good manner, as shown in Fig. 4. Comparisons with experimental data obtained from direct active measurements have shown very good agreement (Amgarou et al., 2003).

3. Proxy equilibrium factor measurements with LR 115

In this section, we propose to use the bare LR 115 detector (12 μm red cellulose nitrate on a 100 μm clear polyester base, from DOSIRAD, Type 2, non-strippable), which is a commonly used SSNTD, for determining the airborne ^{218}Po + ^{214}Po concentration, and show that this concentration can be employed to give good estimates of the equilibrium factor. The LR 115 detector has an upper energy threshold for track formation, which is well below the energy of α-particles emitted by the radon progeny deposited on the detector. In other words, plateout progeny are not detected by LR 115. The present method was previously described in Nikezic et al. (2004). The current section serves as a summary of the method and provides more detailed explanations for some parts.

3.1. Determination of response of LR 115

In the following, we will investigate the response of the bare LR 115 detector to ^{222}Rn and its α-emitting short-lived progeny, i.e., ^{218}Po and ^{214}Po. The task is to study the partial sensitivities ρ_i of the detector to radon and its progeny (i.e., the number of tracks per unit area per unit exposure, i.e., the unit of $(\mathrm{m}^{-2})/(\mathrm{Bq\,m}^{-3}\,\mathrm{s})$ or just (m)).

A cross-section of the sampling volume is shown in Fig. 5. The initial points of α-particles in the simulations

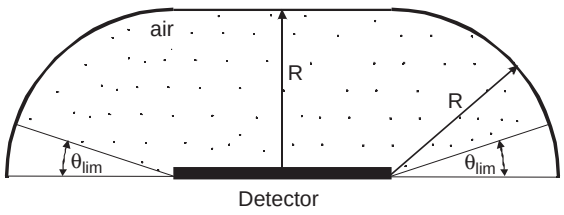

Fig. 5. Cross-section of the sampling volume of initial points of α-particles in the simulation. This figure is adopted from Nikezic et al. (2004). R is range of α-particles in air, while $\theta_{\mathrm{lim}} = \mathrm{asin}(1/V_{\mathrm{max}})$ is critical angle. The 3-D object is obtained by rotation of the curve around the normal onto the detector.

have been chosen in such a way that their distances to the detector are less than the range R of the α-particles in air. They are also chosen so that the incident angle to the detector is larger than the theoretical critical angle $\theta_{\lim}$, which is defined as $\theta_{\lim} = \operatorname{asin}(1/V_{\max})$, where $V_{\max}$ is maximal value of the V function (the ratio of the track etch rate V_t to the bulk etch rate V_b, i.e., $V = V_t/V_b$). Particles striking the detector with an angle smaller than $\theta_{\lim}$ cannot produce any track.

To determine the incident energy of an α-particle when it strikes the detector, the SRIM2000 program (Ziegler, 2001) was employed. The stopping-power data were used to produce energy-distance tables for α-particles in air. The energy E_x of the α-particle incident on the detector after traveling a distance in air was determined by linear interpolation between data in the corresponding energy-distance table. The ranges of α-particles in the LR 115 detector (cellulose nitrate) were also determined using the data obtained from SRIM2000.

We determine the distributions of lengths of major and minor axes of α-tracks in the LR 115 detector produced by ^{222}Rn, ^{218}Po and ^{214}Po. The Monte Carlo program developed earlier by us (Nikezic and Yu, 1999) is employed. The lengths of major and minor axes were calculated by the model recently developed by the present authors (Nikezic and Yu, 2003).

The partial sensitivities depend on the V function ($V = V_t/V_b$) as well as the thickness of the removed active layer during etching. In this section, our objective is to illustrate the concept behind the proposed method. Therefore, in these preliminary calculations, we adopted the V function published by Durrani and Green (1984) as

$$V = 1 + (100\mathrm{e}^{-0.446R'} + 5\mathrm{e}^{-0.107R'})(1 - \mathrm{e}^{-R'}), \qquad (3)$$

where R' is the residual range.

For the time being, we used a removed active layer (i.e., the removed cellulose nitrate layer) of 6.54 μm as an example (taking V_b=3.27 μm h^{-1} and etching for 2 h). The initial thickness of LR 115 was taken as 12 μm as declared by the manufacturer, so the residual thickness of the active layer was 5.46 μm. The bulk etch rate of the LR 115 detector was indirectly determined by many authors in the past (Somogyi et al., 1978; Nakahara et al., 1980) through measurements of track radii after irradiation to fission fragments. Direct measurements of V_b were made recently (Yip et al., 2003). It is also noted that the actual removed active layer varies from sample to sample, and stirring significantly enhances the bulk etch rate (Yip et al., 2003).

In the course of simulations, only the tracks which perforate the active layer of the LR 115 detector are considered. All the tracks were selected according to the lengths of their major and minor axes, with steps of 0.2 μm. When the calculations were completed, the number distribution N_j is obtained, which is the number of tracks within a unit detector area with the length of the major axis between D_j and $D_j + 0.2$ μm. The number distribution is then divided by the total number of the tracks to give the probability distribution p_j, which represents the probability of a particle creating a track with the major axis length between D_j and $D_j + 0.2$ μm. The ratio $p_j/0.2$ is the probability density δ_j (in m^{-1}).

The next step was the multiplication of δ_j with εVCt, where V is the volume (m^3) of the space where the initial points of α-particles were chosen (Fig. 5), C (Bq/m^3) the concentration of α-emitters (radon or radon progeny in our case) in air, ε the detection efficiency expressed as the ratio between the number of particles creating perforated tracks in the detector to the total number of emitted particles, and t (s) is the time of irradiation. Since VCt is the number of α-particles emitted in the time interval t in the space above the detector, εVCt is the number of the tracks created in a unit area of the detector. Therefore, the product $\delta_j \varepsilon VCt$ is the number distribution for the given exposure Ct, i.e., the probability to obtain a track with the major axis in the range $(D, D + \mathrm{d}D)$ for the exposure Ct. We denote this product $\delta_j \varepsilon VCt$ as $(\mathrm{d}N/\mathrm{d}D)$ where N is the number of tracks for a unit detector area. If we assume that $Ct = 1\,\mathrm{Bq\,s\,m^{-3}}$, $(\mathrm{d}N/\mathrm{d}D)$ for a unit exposure and a unit detector area is obtained. The same formulations can be applied for the cases of the minor axis.

3.2. Theoretical results and discussion

Figs. 6 and 7 show the distribution $(\mathrm{d}N/\mathrm{d}D)$ of the major and minor axes of perforated tracks in the LR 115 detector, respectively, for a unit exposure and a unit detector area ($\mathrm{d}N = \delta_j \varepsilon VCt\,\mathrm{d}D = \delta_j \varepsilon V\,\mathrm{d}D$ for a unit exposure). From Fig. 6, the lengths of the major axes are between 6 and 16 μm with two maxima, the more pronounced one being at about 13 μm (longer tracks), and the less pronounced one being at about 9 μm (shorter tracks). From Fig. 7, the lengths of the minor axes are between 2.5 and 13 μm also with two maximums, the more pronounced one being at about 6 μm (narrower tracks), and the less pronounced one being at

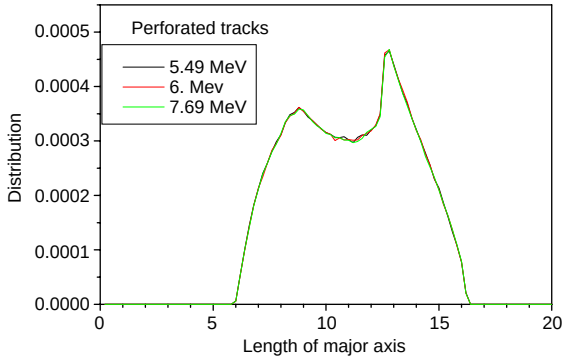

Fig. 6. Distribution (see text for definition) of the length of major axes for perforated tracks in LR 115.

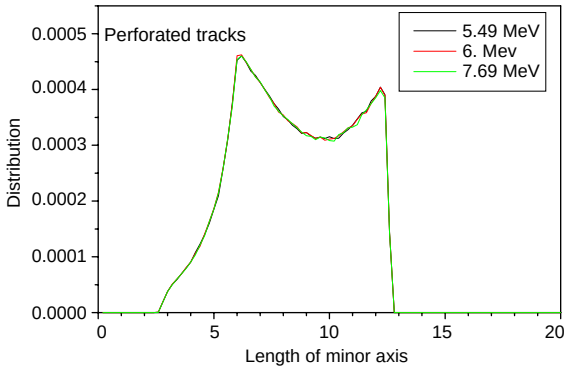

Fig. 7. Distribution (see text for definition) of the length of minor axes for perforated tracks in LR 115.

about 12 μm (wider tracks). The bimodal distributions can be explained through analyses of angular and energy distribution of α-particles incident on the detector and are related to the track formation model. The peaks corresponding to longer axes are created by α-particles with incident energies between 1.5 and 2.5 MeV, while the peaks corresponding to shorter axes originated from α-particles with incident energies between 3 and 4 MeV.

3.3. Equality of partial sensitivities

It is interesting to observe from Figs. 6 and 7 that the curves $(\mathrm{d}N/\mathrm{d}D)_i$ for three α-energies i in the radon chain overlap completely for the entire ranges of the length for both major and minor axes. From this result, we see that $\rho_i = \int (\mathrm{d}N/\mathrm{d}D)_i \, \mathrm{d}D$ are the same for different i, where ρ_i is the number of tracks on a unit detector area for a unit exposure to the α-energy i in the radon chain, or in short, the partial sensitivity for i. In other words, the partial sensitivities ρ_i of the LR 115 detector to ^{222}Rn, ^{218}Po and ^{214}Po are the same. It is remarked here that the equality of partial sensitivities arises because of the presence of the upper energy threshold for recording α-particle tracks in LR 115. For other detectors without the upper energy threshold, e.g., CR-39, the partial sensitivities will not be the same.

The equality among the partial sensitivities is an interesting result. Similar results have been obtained by previous research but the phenomenon has not been studied in details and has not been explained. For example, Somogyi et al. (1984) found that partial sensitivities in diffusion chambers were equal among themselves if the radius of chamber was larger than 4 cm, and if the progeny were not deposited onto the chamber wall. Under such conditions, the detector operated just like a bare one. The value given by Somogyi et al. (1984) for partial sensitivity was about 0.28×10^{-2} m (as recalculated by the present authors using data from the graph in the original work). Nikezic and Baixeras (1996) calculated partial sensitivities of a bare detector as a function of the removed layer and found that they were very close to each other for the same thickness of removed layer. At that time, they applied the track growth model of Somogyi and Szalay (1973) and got the value $\rho_i = 0.244 \times 10^{-2}$ m for 6 μm of removed layer and $\rho_i = 0.334 \times 10^{-2}$ for 7 μm of removed layer. Linear interpolation gives $\rho_i \approx 0.29 \times 10^{-2}$ m, which is close to the value of 0.288×10^{-2} m obtained here with our model of the track growth. Different models of track growth brought close results for partial sensitivities.

3.4. Equilibrium factor determination

By integration of the corresponding $(\mathrm{d}N/\mathrm{d}D)_i$ curves in Figs. 6 and 7, we found that the partial sensitivities ρ_i are

$$\rho_i = \rho_{^{222}\mathrm{Rn}} = \rho_{^{218}\mathrm{Po}} = \rho_{^{214}\mathrm{Po}} = 0.288 \times 10^{-2}\ \mathrm{m}. \quad (4)$$

Therefore, the total sensitivity in the case of radioactive equilibrium between radon and its progeny will be $\rho_{^{222}\mathrm{Rn}} + \rho_{^{218}\mathrm{Po}} + \rho_{^{214}\mathrm{Po}} = 0.864 \times 10^{-2}$ m. In case of disequilibrium, the total track density ρ (in track/m^2) on the detector is

$$\rho = \rho_i (C_0 + C_1 + C_3) t, \quad (5)$$

where C_0, C_1 and C_3 are concentrations of ^{222}Rn, ^{218}Po and ^{214}Bi(Po) in Bq/m^3 and t is the exposure time. If the radon concentration C_0 is known (e.g., from a separate measurement), we can obtain the sum $(C_1 + C_3)$ given as

$$C_1 + C_3 = \frac{\rho}{\rho_i t} - C_0. \quad (6)$$

Dividing by C_0, this becomes

$$F_\mathrm{p} = f_1 + f_3 = \frac{C_1}{C_0} + \frac{C_3}{C_0} = \frac{\rho}{\rho_i t C_0} - 1, \quad (7)$$

where F_p is a sum of f_1 and f_3, and is given the name "proxy equilibrium factor" (Nikezic et al., 2004).

As it was mentioned above, a similar quantity, called the reduced equilibrium factor F_red, introduced recently by Amgarou et al. (2003) was defined in Eq. (2). It has been shown that the equilibrium factor can be determined if F_red is known. Amgarou et al. (2003) calculated equilibrium factors through the Jacobi (1972) room model by systematically varying all parameters that influence the concentrations of radon and its progeny, and plotted them with F_red. We repeat the procedures here, but replace F_red with F_p, and the results are shown in Fig. 8 (which is in fact equivalent to Fig. 1 of Amgarou et al. (2003) with a shift of one unit). It is observed that the proxy equilibrium factor has a good correlation with the equilibrium factor F (although not as good as the correlation between F_red and F) so we have effectively found a convenient method for the determination of F with the LR 115 detector. The method proposed by Amgarou et al. (2003) through the reduced equilibrium factor F_red involved measurements of ^{218}Po and ^{214}Po concentrations.

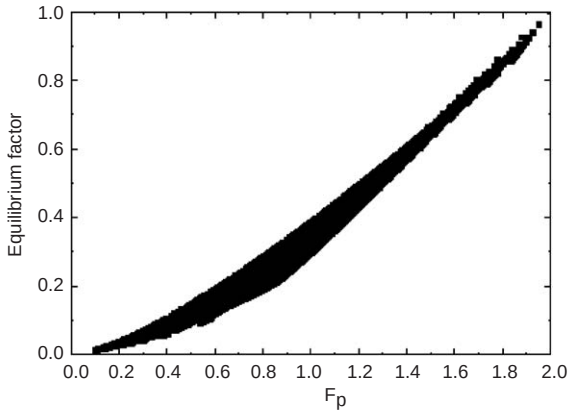

Fig. 8. Dependence of the equilibrium factor F on the proxy equilibrium factor $F_p(=f_1+f_3)$.

Table 1
The three exposure conditions in the radon exposure chamber

	Exposure 1	Exposure 2	Exposure 3
Duration of exposure (h)	71.9	72	72
Average ^{222}Rn concentration (Bq m^{-3})	854	1066	1643
Average equilibrium factor	0.76	0.21	0.13

4. Experimental validation

4.1. Exposure of LR 115 detectors

LR 115 detectors (12 μm red cellulose nitrate on a 100 μm clear polyester base, from DOSIRAD, Type 2, non-strippable) with a size of $3\times3\,cm^2$ were exposed in a radon exposure chamber (with a volume of 1.46 m^3) under different concentrations of radon and radon progeny, the details of which are summarized in Table 1. For this preliminary experimental validation, only two LR 115 detectors were used for each of the three exposures. A higher number would have allowed to reduce uncertainties.

The radon exposure chamber (Leung et al., 1994) was filled with ^{222}Rn generated from a 22.9 kBq ^{226}Ra source in a flow through mode at a flow rate of about 3.1 L min^{-1}. The ^{222}Rn concentration inside the chamber was measured by a continuous ^{222}Rn monitor while the equilibrium factor of ^{222}Rn progeny was adjusted by controlling the total aerosol concentration, which would drop quite rapidly due to the circulation and the plateout effect. Hence to maintain a certain aerosol concentration and equilibrium factor inside the chamber, aerosols with a median diameter of about 150 nm produced by an aerosol atomizer were injected regularly into the radon chamber to maintain the equilibrium equivalent concentration of the airborne ^{222}Rn progeny. The total aerosol concentration inside the chamber was intermittently monitored by a scanning mobility particle sizer which indicated that the aerosol concentration could be maintained quite steadily by controlling the injection duration of the aerosols and period of the injections. The ^{222}Rn progeny inside the radon chamber were measured by collecting them on a 47 mm diameter member filter at a flow rate of about 11 L min^{-1}. The sampling time was 30 min. The α-emissions from the collected progeny were read by a ZnS scintillator and a photomultiplier tube/counter system. By using the 3-count method (Thomas, 1972), the PAEC, EEC and hence the equilibrium factor of the progeny were calculated. Since sampling of ^{222}Rn progeny at high flow rates would significantly altered the equilibrium factor inside the chamber, only grab sampling method was used and this was done twice a day.

Once the required exposure condition inside the chamber was reached, the LR 115 detectors were transferred into the chamber through an airlock for exposure. The films were exposed for about 3 days and then taken out of the chamber for chemical etching.

4.2. Etching and measurements of active layer thickness

The exposed LR 115 detectors were etched in 2.5 N aqueous solution of NaOH at 60 °C. The temperature was kept constant with an accuracy of ±1 °C. The detectors were etched using a magnetic stirrer (Model No: SP72220-26, Barnstead/Thermolyne, IA, USA) for more uniform etching (Yip et al., 2003). After etching for ∼ 60 min, the detectors were taken out of the etchant, rinsed with deionized water and dried.

For each detector, a small part of the active layer was peeled off from the polyester base to form a step, which was then used to reveal the thickness of the active layer by surface profilometry measurements (Yip et al., 2003). A surface profilometry system called Form Talysurf PGI (Taylor Hobson, Leicester, UK) was employed in the present work. The measuring system is based on a laser interferometric transducer. A computer-controlled stylus passes slowly across a surface of interest during measurements, while the data are processed by the computer to generate an output graph showing the profile of the scanned surface. The mean value and the standard deviation for the active-layer thickness were obtained through measurements for five different positions of the step.

4.3. Determination of equilibrium factor

The partial sensitivity ρ_i involved in the present technique is crucially dependent on the removed active layer thickness, the latter being variable in real-life measurements. In

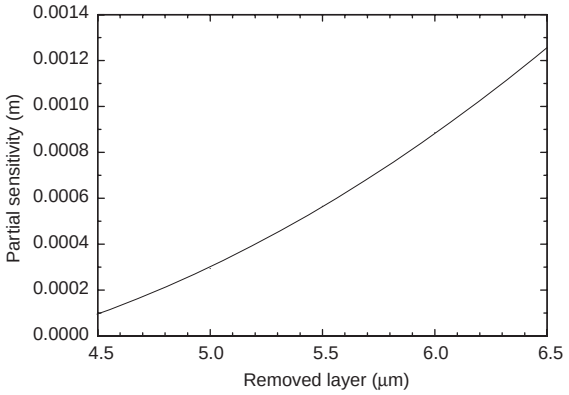

Fig. 9. The relationship between the partial sensitivity of the LR 115 detector from DOSIRAD and the removed active layer thickness.

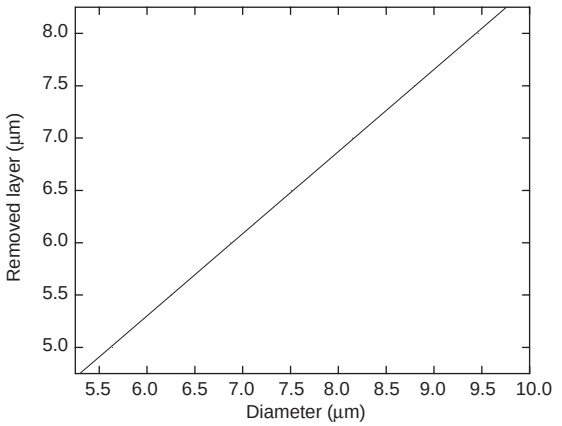

Fig. 10. Relationship between the removed active layer and the track diameter of normally incident 3 MeV α-particles.

order to obtain more accurate values for the partial sensitivity ρ_i, the theoretical relationship between ρ_i and the removed layer should be derived through computer simulations. Furthermore, this relationship should be derived for the V function determined for the actual detectors being used, which is the LR 115 detector from DOSIRAD in our case. Fig. 9 shows such a relationship between the partial sensitivity of the LR 115 detector from DOSIRAD and the removed active layer thickness.

From the measured removed active layer thickness of our detectors, the partial sensitivities have been determined from Fig. 9. The partial sensitivities thus determined for our detectors are shown in Table 2, together with the determined track densities, as well as the derived values of F_p and F. The experimental values of F (obtained using Fig. 8) are also given for a comparison. From the results, we can see that the derived values of F are in excellent agreement with the experimental values, except probably detector 6.

For researchers who would like to use the present method for long-term measurements of the equilibrium factor, but who do not have some convenient equipment (such as surface profilometry systems) to accurately and conveniently measure the thickness of the removed active layer, we have also provided here a curve showing the theoretical relationship between the removed active layer thickness and the track diameter of normally incident 3 MeV α-particles in Fig. 10 (by using the V function for LR 115 detectors). Before the exposure of an LR 115 detector to the environment, the detector is irradiated with normally incident 3 MeV α-particles, e.g., from an ^{241}Am source, by using a collimator. The irradiated area is then masked, e.g., by using rubber cement. After exposure to the environment for a predetermined period of time, the mask is removed, and the detector is etched until the diameter of the tracks from the normally incident 3 MeV α-particles has reached a desired value. The removed layer is then read from Fig. 10, and the partial sensitivity can then be read from Fig. 9.

5. Conclusion and discussion

A method has been introduced for the determination of the equilibrium factor using the bare LR 115 detector by exploiting the equal partial sensitivities ρ_i of the LR 115

Table 2
The partial sensitivities and track densities determined for our detectors, and the derived values of F_p and F

Detector	Partial sensitivity (10^{-4} m)	Track density (10^6 m^{-2})	F_p	Calculated F	Experimental F
1	1.960	0.124	1.80	0.83–0.88	0.76±0.14
2	3.710	0.221	1.69	0.75–0.80	0.76±0.14
3	3.108	0.171	0.81	0.18–0.31	0.21±0.06
4	3.532	0.168	0.57	0.08–0.18	0.21±0.06
5	4.625	0.245	0.54	0.07–0.17	0.13±0.04
6	3.572	0.182	0.09	0.00–0.03	0.13±0.04

The experimental values of F (with errors corresponding to 1 standard deviation) are also given for a comparison.

detector to ^{222}Rn and its α-emitting short-lived progeny, ^{218}Po and ^{214}Po. A proxy equilibrium factor F_p is defined as $(f_1 + f_3)$, i.e., the ratio between the sum of concentrations of the two α-emitting radon progeny (^{218}Po + ^{214}Po) to the concentration of ^{222}Rn gas. Due to the equal partial sensitivities, $F_p = (\rho/\rho_i t C_0) - 1$, where ρ (track/m^2) is the total track density on the detector, t is the exposure time, C_0 (Bq/m^3) is the concentration of ^{222}Rn, and ρ_i can be calculated from the V function and the removed active layer of the LR 115 detector. If C_0 is known, we can obtain F_p which is well correlated with the equilibrium factor. This leads to a novel method for long-term determination of the equilibrium factor. The method has been verified by experiments.

Acknowledgements

The present research is supported by the CERG Grant CityU1081/01P from the Research Grant Council of Hong Kong.

References

Amgarou, K., Font, L., Baixeras, C., 2003. A novel approach for long-term determination of indoor ^{222}Rn progeny equilibrium factor using nuclear track detectors. Nucl. Instrum. Meth. A 506, 186–198.

Dorschel, B., Piesch, E., 1993. A new approach to estimating the equilibrium factor between radon and its daughters. Radiat. Prot. Dosim. 48, 145–151.

Durrani, S.A., Green, P.F., 1984. The effect of etching conditions on the response of LR115. Nucl. Tracks 8, 21–24.

Fleischer, R.L., 1984. Theory of passive measurement of radon daughters and working levels by the nuclear track technique. Health Phys. 47, 263–270.

Frank, A.I., Benton, E.V., 1977. Radon dosimetry using plastic nuclear track detectors. Nucl. Track Det. 1, 149–179.

Hadler, J.C., Paulo, S.R., 1994. Indoor radon daughter contamination monitoring: the absolute efficiency of CR-39 taking into account the plateout effect and environmental conditions. Radiat. Prot. Dosim. 51, 283–296.

Jacobi, W., 1972. Activity and potential energy of ^{222}Rn and ^{220}Rn daughters in different air atmosphere. Health Phys. 22, 441–450.

Leung, J.K.C., Jia, D., Tso, M.Y.W., 1994. A fully automated radon exposure Chamber. Nucl. Instrum. Meth. A 350, 566–571.

Lubin, J.H., Boice Jr., J.D., Edling, C., Hornung, R.W., Howe, G., Kunz, E., Kusiak, R.A., Morrison, H.I., Radford, E.P., Samet, J.M., Tirmarche, M., Woodward, A., Yao, S.X., Pierce, D.A., 1995. Lung cancer in radon-exposed miners and estimation of risk from indoor exposure. J. Nat. Cancer Inst. 87, 817–827.

Muirhead, C.R., 1997. In: Durrani, S.A., Ilic, R., (Eds.) Radon Measurements by Etched Track Detectors: Applications to Radiation Protection, Earth Sciences and the Environment. World Scientific, Singapore, pp. 243–257.

Nakahara, N., Kudo, H., Akiba, F., Murakami, Y., 1980. Some basic studies on the absolute determination of radon concentration in the air by a cellulose nitrate track detector. Nucl. Instru. Meth. 171, 171–179.

Nikezic, D., Baixeras, C., 1996. Radon radon progeny and equilibrium factor determination using an LR115 detector. Radiat. Meas. 26, 203–213.

Nikezic, D., Yu, K.N., 1999. Determination of deposition behaviour of ^{218}Po from track density distribution on SSNTD in diffusion chamber. Nucl. Instrum. Meth. A 437, 531–537.

Nikezic, D., Yu, K.N., 2002. Incidence characteristics of alpha particles on detectors irradiated in a radon + progeny atmosphere. Nucl. Instrum. Meth. B 187, 492–498.

Nikezic, D., Yu, K.N., 2003. Three-dimensional analytical determination of the track parameters: over-etched tracks. Radiat. Meas. 37, 39–45.

Nikezic, D., Yu, K.N., 2004. Formation and growth of tracks in nuclear track materials. Materials Science and Engineering R 46, 51–123.

Nikezic, D., Ng, F.M.F., Yu, K.N., 2004. Theoretical basis for long-term measurements of equilibrium factors using LR 115 detectors. Applied Radiation and Isotopes 61, 1431–1435.

Nikolaev, V.A., Ilic, R., 1999. Etched track radiometers in radon measurements: a review. Radiat. Meas. 30, 1–13.

NRC (National Research Council), 1999. Health effects of exposure to radon. National Academic Press, Washington, DC.

Planinic, J., Faj, Z., 1990. Equilibrium factor and dosimetry of Rn by a nuclear track detector. Health Phys. 59, 349–351.

Somogyi, G., Hunyadi, I., Varga, Z., 1978. Spark counting of α-radiograms recorded on LR-115 strippable cellulose nitrate film. Nucl. Track Det. 2, 191–197.

Somogyi, G., Paripas, S., Varga, Z., 1984. Measurement of radon, radon daughters and thoron concentrations by multi-detector devices. Nucl. Tracks Radiat. Meas. 8, 423–427.

Somogyi, G., Szalay, S.A., 1973. Track-diameter kinetics in dielectric track detectors. Nucl. Instru. Meth. 109, 211–232.

Thomas, J.W., 1972. Measurement of radon daughters in air. Health Phys. 23, 783–786.

Yip, C.W.Y., Ho, J.P.Y., Koo, V.S.Y., Nikezic, D., Yu, K.N., 2003. Effects of stirring on the bulk etch rate of LR 115 detector. Radiat. Meas. 37, 197–200.

Ziegler, J.F. 2001, SRIM-2000, http://www.srim.org/.